INTERIM REPORT
U.S. Department of Energy

NOVEL MINIATURE SPECTROMETER FOR REMOTE CHEMICAL DETECTION

Principal Investigator: Dr. Andrew C. R. Pipino
National Institute of Standards and Technology (NIST)
Gaithersburg, MD 20899-8363

Project Number: 60231
Grant Number: DE-AI07-97ER62518
Grant Project Officers:
Dr. Matesh N. Varma
Mr. Gordon Roesler
Project Duration: 9/15/97 - 9/14/00

Table of Contents

1. Executive Summary

The development of new chemical sensing technologies is critical to the DOE environmental management effort. New sensing technologies are needed to identify and quantify contaminants under a wide range of conditions, including extremely hazardous environments. New durable sensors are also needed for long-term monitoring of contaminated sites. Indeed the enormity, complexity, and toxicity of DOE sites has created uniquely demanding requirements for new sensing technologies.

Project# 60231 has yielded a new technology that has the potential to enable qualitative and quantitative remote, real-time, optical diagnostics of chemical species in hazardous gas, liquid, and semi-solid phases. The technology employs a miniature optical resonator formed from a cube or polygon of an ultra-pure optical solid, which can be immersed in the environment of interest. A light pulse circulates within the solid resonator, probing the presence of chemical species at the resonator surfaces. These miniature resonators form the basis for a new chemical detection technique, termed evanescent wave cavity ring-down spectroscopy (EW-CRDS).

At the beginning of Project 60231, EW-CRDS was mostly a concept that was supported by theoretical calculations and some preliminary experimental results. During year 1, the first miniature, square, total-internal-reflection (TIR)-ring resonator experiments were successfully demonstrated. During year 2, the chemical detection sensitivity and light polarization properties where elucidated. Both wavelength and polarization dependence were employed for identification and quantification of a molecular species of interest in prototype experiments. Also in year 2, the monolithic,

folded resonator and hexagonal TIR-ring resonator designs were developed and fabricated. During year 3, the monolithic folded and hexagonal TIR-ring resonator designs were characterized and the use of diode lasers for CRDS measurements was explored. Over the course of the project, three patents and four publications were produced.

Concerning relevance, impact, and technology transfer, the EW-CRDS technology has the potential to fulfill many of DOE's sensing needs by ultimately providing a sensitive, selective, and rugged *in-situ* chemical sensing technology that is patent-protected and currently licensed. Project #60231 has demonstrated feasibility of the new sensing concept and begun to provide a thorough understanding of the fundamental measurement science underlying the technology. Such fundamental knowledge is essential to assuring accuracy and to allow specific devices to be tailored to specific needs. A rugged *in-situ* probe could dramatically reduce the cost currently associated with sample extraction and *ex-situ* analysis of DOE waste. EW-CRDS also provides a new sensing platform for testing chemically selective films that show molecular recognition for specific analytes of interest to DOE thereby potentially supporting other DOE-funded research. Furthermore, since the miniature resonators used in EW-CRDS can be fabricated from silica, the technique could be used to probe fundamental chemical interactions on silica which are relevant to understanding soil chemistry at DOE sites.

The development of EW-CRDS is in its infancy. More basic research is needed to understand the role of the nascent resonator surface in the adsorption/collection of

analyte and to explore the potential for characterizing chemically selective films and silica chemistry in the environment. Other spectral regions, optical materials, and modes of operation (such as ellipsometric sensing) should also be explored. For the current status of commercialization and patent licensing, contact Terry Lynch at NIST (301-975-2691).

2. Research Objectives

New chemical sensing technologies are critically important for addressing many of EM's priority needs as discussed in detail at http://emsp.em.doe.gov/needs. Many *technology needs* were addressed by this research. For example, improved detection strategies are needed for non-aqueous phase liquids (NAPL's), such as PCE ($Cl_2C=CCl_2$) and TCE ($HClC=CCl_2$), which persist in the environment due their highly stable structures. By developing a miniature, ultra-sensitive, selective, and field-deployable detector for NAPL's, the approximate source location could be determined with minimal investigative expense. Contaminant plumes could also be characterized in detail. The miniature spectrometer developed under Project #60231 could also permit accurate rate measurements in less time, either in the field or the laboratory, which are critically important in the development, testing, and ultimate utilization of models for describing contaminant transport. The technology could also be used for long-term groundwater monitoring or long-term stewardship in general. Many *science needs* are also addressed by the Project 60231, since the effort significantly advances the measurement science of chemical detection.

Developed under Project #60231, evanescent wave cavity ring-down spectroscopy (EW-CRDS) is a novel form of CRDS, which is an the emerging optical absorption technique. Several review articles on CRDS, which has been generally applied only to gas-phase diagnostics, have been published[1-3]. EW-CRDS[4-10] forms the basis for a new class of chemical sensors that extends CRDS to other states of matter and leads to a miniaturized version of the concept. EW-CRDS uses miniature solid-state optical resonators that incorporate one or more total internal reflection (TIR) surfaces, which create evanescent waves. The evanescent waves emanate from the TIR surfaces, sampling the surrounding medium. The utility of evanescent waves in chemical analysis forms the basis for the field of attenuated total reflectance (ATR)[11] spectroscopy. Many diagnostic problems can be solved by ATR methods that are intractable by ordinary methods, but ATR typically lacks sensitivity for ultra-trace chemical detection. In EW-CRDS, the ring-down time of a resonator sensitively responds to chemical species present in the evanescent wave thereby combining the advantages of ATR with the sensitivity of CRDS. Furthermore, EW-CRDS forms the basis for a rugged miniature chemical sensor for which the laser source and photodetector can be located remotely by using optical fiber. Work on EW-CRDS began at NIST with the NRC postdoctoral associateship of the current Principal Investigator during fiscal 1996-1997. Since completion of the NRC associateship, work on EW-CRDS has been majority funded through Project 60231, with some additional funding from the Advanced Technology Program (35K/year in 2000).

3. Methods and Results

A. Background and Preliminary Studies

Chemical sensing can be accomplished by many strategies. In general, optical techniques

offer significant advantages, including high sensitivity, cost-effectiveness, and remote detection. In the shot-noise limit, optical absorption spectroscopy has the potential to be the most sensitive optical technique, since the intrinsic molecular cross-sections are typically largest for absorption. Optical absorption is also the most general optical technique since all molecules absorb light at some frequency. However, to reach the ultimate potential of absorption spectroscopy requires the ability to detect a small power loss in a large optical signal. Some progress in this direction was made years ago with the development of modulation techniques[12,13] in which the intensity or frequency of an optical beam was modulated and detected with a lock-in amplifier, which substantially reduced 1/f noise. A minimum detectable absorption of) I/I~10^{-7} can be achieved with modulation techniques under laboratory conditions, which permits detection of a single molecule of a very strong absorber at very low temperatures[14]. However, in addition to being relatively expensive, modulation techniques are complicated, both in terms of instrumentation and data interpretation.

Recently, with the development of cavity ring-down spectroscopy (CRDS)[1-3], detection of absorption changes of ~10^{-9} has been demonstrated[15], with changes of ~10^{-13} predicted to be possible[16]. Of equal importance, the extremely high sensitivity provided by CRDS is

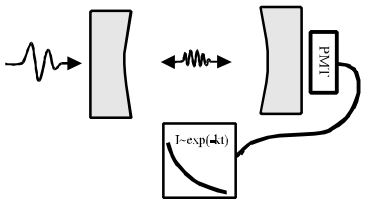

Figure 1. The basic CRDS experiment is depicted. A light pulse is injected into a low-loss optical cavity through a cavity mirror. The residual pulse intensity, which decays exponentially with time, is detected by a photodetector (PMT). The ring-down time, given by Eq. 1, is determined by the intrinsic mirror losses and absorption by gases between the mirrors. Cavity lengths are typically 10-100 cm for this "conventional" CRDS scheme.

obtained with a comparatively simple measurement. Depicted schematically in Figure 1, the CRDS technique uses the intensity decay rate of light pulses injected into a low-loss optical cavity as the absorption-sensitive observable. Typically, the cavity is formed from a pair of ultra-high reflectivity (R>0.9999) concave mirrors configured to form a stable optical resonator. A light pulse circulates with a mean lifetime or "ring-down" time given by,

$$\hat{o}(\grave{u}) \quad \frac{t_r}{L_0(\mathsf{T}) \quad L_{abs}(\mathsf{T})} \qquad \textbf{(1)}$$

where $t_r = 2n_iL/c$ is the round-trip transit time for light in the cavity of length L, $L_0(\mathsf{T})$=1-R accounts for the intrinsic round-trip cavity loss (arising from imperfect mirror reflectivity for the cavity in Figure 1) and $L_{abs}(\mathsf{T})$ arises from sample absorption. The ring-down time is determined by fitting the decaying transmitted light intensity to an exponential function. Determination of absorption is thereby transformed from the measurement of an optical power ratio as in standard absorption spectroscopy to a measurement of time. A complete measurement is accomplished with a single light pulse, thereby eliminating errors introduced

by light source fluctuations. The minimum detectable absorbance change is determined by the product of the intrinsic loss, L_0(T), and the minimum detectable relative change in the ring-down time) J/J, or ("L)$_{min}$=L_0*) J/J. This form for ("L)$_{min}$ reveals the simplicity and challenge of CRDS: Minimize the intrinsic cavity loss and determine the ring-down time with the highest possible precision. The implementation of CRDS depicted in Figure 1 has been generally applied only to gas phase diagnostics. Extending CRDS to condensed phases requires novel cavity designs that allow sampling without the introduction of additional intrinsic losses, resulting from refection losses at interfaces, for example.

To extend CRDS to condensed phases in a general way, EW-CRDS employs the properties of total internal reflection (TIR). For light incident on a perfectly smooth interface between two media with indices of refraction n_i and n_o, TIR occurs when the angle of incidence 2$_i$ exceeds the critical angle, defined by 2$_c$ = $\sin^{-1}(n_i/n_o)$, which in theory provides a perfect (R=1), broadband mirror. In practice, the reflectivity is less than unity due to surface roughness, scattering and nonspecular transmission arising from the non-planar character of real wavefronts. Yet ultra-smooth polished surfaces with root-mean-square surface roughness of ~0.05 nm can be generated routinely for many optical materials, yielding effective mirror reflectivities of R~0.999999 in the visible region of the spectrum. Furthermore, TIR generates an evanescent wave with a locally enhanced surface electric field at the TIR interface, which increases chemical detection sensitivity for molecules that adsorb to the TIR surface.

EW-CRDS combines intra-cavity TIR with CRDS. Initially, Pipino *et al.*[5] constructed a prototype cavity to establish the feasibility of the EW-CRDS concept. Figure 2 shows a schematic diagram of the cavity, which employs a precision-fabricated, super-polished, fused-silica Pellin-Broca prism. The Pellin-Broca prism permits high-transmission of light over a narrow range of wavelengths around the design wavelength (633 nm in this case), if the light is polarized in the plane of the prism and incident at Brewster's angle. A right-angle

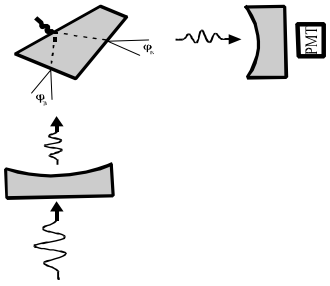

Figure 2 . A low-loss optical cavity is shown which incorporates intra-cavity TIR. Light enters and exits the Pellin-Broca prism at Brewster's angle to minimize Fresnel reflection losses. The prism was fabricated with an accuracy of 3 arc-min from high-purity fused-silica with an estimated bulk attenuation of 50 ppm/cm. The surfaces are super-polished to <0.05 nm RMS surface roughness. The mirrors were commercially available, nominally 99.99% reflective, with a peak reflectivity at 620 nm. The cavity yields a minimum detectable absorbance change of ~32×10^{-6}.

cavity geometry results because light enters and exits the prism at Brewster's angle and undergoes TIR at an intermediate surface with a 45^o angle of incidence. A total round-trip loss of 6.4×10^{-3} was found for this cavity, which yielded a ~ 1 microsecond ring-down time and a minimum detectable absorbance change of 32×10^{-6}, given the 0.5% ring-down time measurement precision for these experiments. In comparison, the linear cavity results obtained using the same mirrors in the configuration of Figure 1, yielded a round-trip loss of 0.67×10^{-3}, indicating an increase of approximately a factor of 10 due to the prism. This

increase in intrinsic loss can be accounted for in terms of depolarization due to residual birefringence and bulk attenuation. Although the Pellin-Broca design served as an important demonstration of the feasibility of EW-CRDS, providing a detection limit of 4 % of a monolayer of adsorbed I_2 at the TIR surface, this design suffers from severe limitations.

B. Innovations and Results of Project 60231

I. Total-internal-reflection-ring resonator

Project #60231 has yielded several new resonator designs for EW-CRDS that circumvent the limitations of the early prototype design, while providing the potential for a single-ended probe. Figure 3 shows a square, TIR-ring cavity, which is a specific example of a general class of polygonal, TIR-ring resonators. The square, TIR-ring design is the simplest fused-silica resonator that sustains optical modes by TIR from the ultra-violet to the near-infrared region. Note that one facet is convex to create a stable resonator, which refocuses the internally circulating light on each round trip. In general, the angle of incidence for a regular, polygonal TIR-ring cavity with n facets is given by 2_i=B(n-2)/2n. For a judicious choice of n, the condition $2_i > 2_c$ is fulfilled by a single 2_i for the full

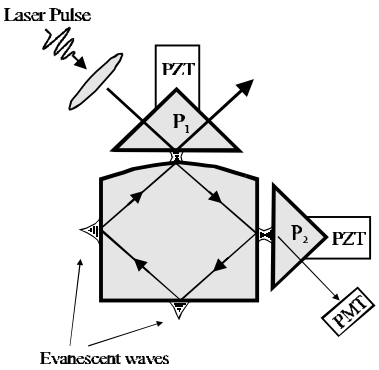

Figure 3. A TIR-ring minicavity is depicted that extends CRDS to condensed phases. The cavity is fabricated from ultra-high-transmission optical material in the form of a regular polygon with a convex facet that refocuses the internally circulating light, forming a stable optical resonator. Light enters and exits the ring by photon tunneling through prisms, P_1 and P_2, which are positioned with piezoelectric translators (PZT) in the prototype experiments. The extremely small round-trip optical loss results in long ring-down times, which are highly sensitive to absorbing media in the evanescent fields emanating from the remaining facets. This work is published in *Physical Review Letters*, (Ref 8).

transmission range of a given optical material, providing a broad spectral range of application. Photon tunneling across the junctions between the monolithic cavity and the coupling prisms P_1 and P_2 is used to excite and monitor the modes, respectively, since direct excitation of a cavity mode by a propagating wave is not permitted for the TIR-ring. The dependence of coupling efficiency and cavity round-trip loss on the tunneling junction gap width was investigated by using piezoelectric translators to provide precise (±5 nm) control of the gap and interferometry to determine the gap size. At the impedance-matched condition where the round-trip loss equals the coupling loss, the on-resonance transmission is near unity. At larger gap widths, the round-trip loss approaches a constant, maximum value, where coupling losses are small relative to other losses. Operation in the weakly coupled region therefore maximizes and stabilizes the ring-down time with respect to variations of the tunneling junction. The relationship between the ring-down time and sample absorbance for the TIR-ring cavity is described by Equation 1 with $L_0(T) = L_{bulk} + L_{diff} + L_{surf} + L_{nspec} + L_{coup}$, where the L_i correspond to bulk, diffraction, surface scattering, non-specular, and coupling losses, respectively. A general theoretical analysis of TIR-ring cavities was presented by Pipino *et al*.[4] With proper material selection and cavity design, $L_0(T)$ can be in the range of $1x10^{-7} \# L_0 \# 1x10^{-3}$ over broad spectral regions, yielding long

ring-down times that can be measured with high precision.

Figure 4 shows single-shot ring-down traces with decay times of 1.270 µs and 1.278 µs for s- and p-polarized cavity modes, respectively, obtained at 580 nm for a 7 mm x 7 mm x 5 mm fused-silica square cavity with a 2.23 cm radius of curvature convex facet [8]. An

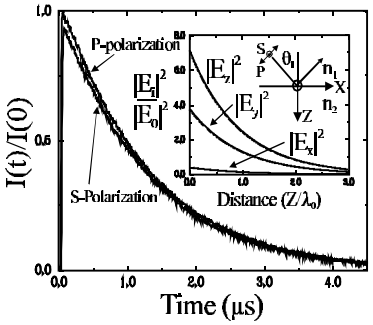

Figure 4. Ring-down traces for s- and p-polarized modes of a fused-silica, square-TIR-ring minicavity are shown for a single laser pulse at 580 nm, where the s-polarized decay is slightly offset for presentation purposes. The cavity modes incur a fractional loss of only ~80 x 10^{-6} per round-trip. The inset shows the electric field intensity components of the evanescent wave calculated using the Fresnel equations as a function of distance from a cavity facet relative to the incident intensity. The surface coordinate system is also shown. Knowledge of surface field direction and magnitude allows molecular orientation to be probed for an absorbing molecule at the surface.

excimer-pumped, pulsed dye laser, which generated 20 ns, ~ 1 mJ pulses, was used as the excitation source without mode matching. The decay waveforms were detected with a photomultiplier tube and an 8-bit digital oscilloscope. At 580 nm, L_0 = 80 x 10^{-6}, which yields a minimum detectable absorption of $\alpha_{min} \approx 1.6 \times 10^{-7}$, given a relative uncertainty in the decay time of 0.2% or better. Yet even at 450 nm, a ring-down of ~200 ns for this cavity remains sufficiently long to permit absorptions of ~1x10^{-6} to be detected. Above 600 nm, the bulk losses of fused silica decrease substantially, reaching a minimum of ~5x10^{-7} cm^{-1} in the near-IR, where extremely high sensitivity measurements can be anticipated.

Since both in-plane (p) and out-of-plane (s) polarizations have high finesse for the TIR-ring cavity, control of polarization allows the electric field intensity distribution at the TIR surface to be varied, permitting a rich variety of polarization dependent phenomena to be probed. The inset in Figure 4 defines the surface coordinate system and shows the calculated components of the electric field intensity of the evanescent wave as a function of distance from a cavity facet[11]. An understanding of the magnitude and direction of the field intensity is essential for interpreting optical absorption by a surface-adsorbed molecule, since only an optical field component that is parallel to the molecular transition dipole moment will be absorbed. By combining knowledge of the electric field intensity with the measured dichroic ratio of s- to p-polarized absorptions, $D=A_s/A_p$, molecular orientation at the surface can be determined, which provides additional selective chemical information. From the inset in Figure 4, the x, y, and z components of the field intensity, $|E_x|^2$, $|E_y|^2$, and $|E_z|^2$, at the TIR surface (z=0) are seen to be modified by factors of 0.4112, 3.783, and 7.154, respectively, relative to the incident field intensity. The p-polarized cavity mode, which is composed of E_x and E_z, is dominated by the strongly enhanced z-component that is normal to the cavity facet, while the s-mode is composed of E_y only, which lies in the plane of the TIR surface. Figure 5 shows ring-down traces for s- and p-polarized modes under identical conditions with Figure 5, but a TIR facet has been exposed to I_2 vapor[17], which has a visible X7B

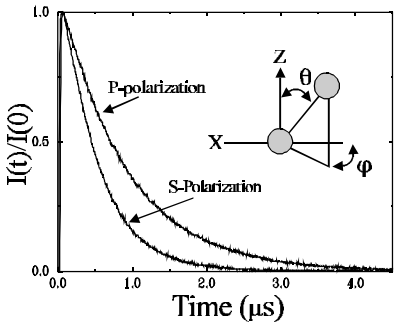

Figure 5. Ring-down traces for s- and p-polarized modes for the identical conditions of Figure 4, but a TIR facet of the resonator has been exposed to I_2 vapor at ambient temperature. Both polarizations show a change in ring-down time, but a larger change for the s-polarized mode suggests that I_2 molecules lie flat on the surface, since the electric field for this mode is parallel to the surface. The inset shows the coordinates for describing orientation. The base ring-down time of Figure 4 is regained with removal of the I_2 source.

transition dipole moment that is aligned with the molecular axis. The inset in Figure 5 shows the polar and azimuthal angles, 2 and N, respectively, for describing orientation of an adsorbed diatomic molecule. Note that both s- and p-polarized modes show a change in ring-down time with J_s=0.497 μs and J_p=0.889 μs, but the s-polarized mode shows a significantly larger change, despite the smaller field enhancement associated with E_y, suggesting that I_2 molecules are preferentially oriented with their molecular axes parallel to the surface. This anisotropic optical response provides an additional signature for an analyte molecule of interest. Furthermore, chemically modified surfaces that show molecular recognition are frequently synthesized from self-assembled monolayers (SAM's), which are highly ordered and oriented systems.

To describe orientation quantitatively, a distribution function N(2,N) is typically invoked[18]. A common strategy is to expand N(2,N) in spherical harmonics, reducing the measurement to a determination of expansion coefficients d_{lm}. In general, optical absorption measurements of the dichroic ratio yield only the value of d_{20}, which is often referred to as the "order parameter". N(2,N) is frequently assumed to be isotropic in n and symmetric in 2, leading to the interpretation of d_{20} in terms of an average polar angle 2_{avg}, obtained from $d_{20}=(3\cos^2 2_{avg} - 1)/2$. From the results of Figures 4 and 5, $d_{20} = -0.50$ is found, which yields $2_{avg}=90^o$, corroborating the qualitative conclusion that I_2 lies flat on the resonator surface. Although for a given value of the order parameter, many distribution functions are actually possible, differing in shape, width, and most-probable angle, it is unlikely that two molecules will show the same absorption and optical anisotropy at a given probe wavelength.

Knowledge of molecular orientation is also required to quantify surface coverage. The absorption cross-section for the surface-bound species is also required, but is generally not known. Iodine served as a suitable probe molecule because the gas-phase peak absorption cross-section at 520 nm of 2.56×10^{-18} cm^2/molecule[19] does not change substantially with physisorption[20]. Assuming I_2 is physisorbed and lies flat on the surface, an estimated minimum detectable coverage of ~0.006 % of a monolayer (1 monolayer = 4.5×10^{14} sites/cm^2) is estimated, based on a minimum detectable absorption of 1.9×10^{-7} achieved for a 25 laser shot average, which provides a relative standard deviation in J of 0.2 % that is instrumentation-limited in the present work. To obtain the highest sensitivity, excitation of a single transverse cavity mode, *e.g.*, TEM_{00}, must be employed to improve decay time precision[21].

In addition to the square, fused silica TIR-ring cavity of Figure 3, a sapphire hexagonal TIR-ring cavity has also been fabricated and tested that could allow liquid samples to be probed by direct immersion. Shown schematically in Figure 6, the hexagonal cavity has a 60^0 angle of incidence at the TIR surface. Taking the refractive index of sapphire as n_i=1.78 and assuming the angle of incidence exceeds the critical angle by at least 2^0, liquids with a refractive index of up to n_o=1.5 can be probed with this resonator design. The c-axis of the sapphire crystal is orthogonal to the resonator plane, which results in separate refractive indices but identical beam paths for s- and p-polarizations. The resonator facets are super-polished to 0.05 nm rms roughness, which reduces the surface scattering loss to ~$1x10^{-6}$ (1 ppm) per surface at 550 nm. Published bulk attenuation data for sapphire shows wide variation based on the crystal growth process and sample history, lacking the substantial effort afforded to fused silica due to communications needs.[22] Our preliminary experiments indicate a 250 ppm/cm loss at 550 nm, although this figure is an upper bound. Because a large difference exists between the critical angle at an air/sapphire interface (~34^0) and the angle of incidence for the hexagonal resonator, a very small tunneling junction (<<ë) is needed for input- and output-coupling when an air-filled gap is employed. Input coupling at the apex of the convex surface is easily achieved, since a small gap can be readily obtained

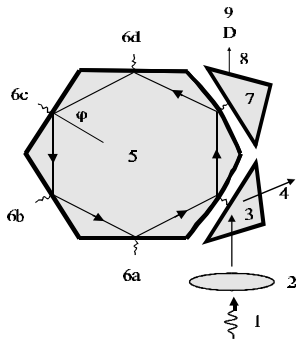

Figure 6. A sapphire, hexagonal resonator has been successfully fabricated and tested. Since sapphire is an extremely hard, durable material, a sapphire sensor would be ideal for a field-deployable device. In general for an n-sided polygonal resonator, as n is increased the surface scattering loss per surface is reduced due to the larger angle of incidence, 2_i=B(n-2)/2n. Sensitivity is enhanced because the number of possible sampling points is increased (% n-2).

between the apex and the flat surface of the input coupling prism. However, output coupling requires two macroscopic (~ 10 mm^2) flat surfaces to be positioned with a small fraction of a wavelength of each other. This was difficult to achieve due to the limited resolution of the manual positioners that controlled other degrees of freedom (tilt, rotation, *etc*.). To circumvent this problem, a liquid (ethylene glycol) was used to fill the coupling junction in order to extend the evanescent wave by reducing the index discontinuity of the junction. Although this effect complicated the prototype experiments, it will ultimately benefit the fabrication of a field-deployable instrument for liquids, since a low-loss thin-film coating or cement can be can be used to fill the coupling junction. With improvements expected, the estimated detection limit for the prototype system is ~1 ppm, based on a digitizer-limited ring-down time precision of 0.2%. These preliminary results suggest that a field-deployable device based on a sapphire resonator may be feasible, which could provide an extremely durable sensor. However, recent experiments performed at Research Electro-Optics Inc. (Boulder, CO), have indicated that undoped YAG may have higher transmission than sapphire, with no birefringence, and yet still have a comparable hardness and refractive index.

ii. Monolithic folded resonator

Since the polygonal, TIR-ring resonators employ only TIR mirrors, a broad spectral bandwidth is accessible. However, since photon tunneling is required to excite and detect the cavity modes, coupling prisms must be employed, which require precise positioning and mounting. This engineering challenge is being addressed in collaboration with our commercial partner. To facilitate the investigation of specific applications of EW-CRDS, another monolithic resonator design for EW-CRDS has been developed, which does not employ photon tunneling. Published in *Applied Optics* (Ref. 9), the monolithic, folded resonator, which is shown in Fig. 7, employs both ultra-high reflective coatings and TIR. Although a restricted bandwidth results from the use of reflective coatings, the design has several advantages including direct excitation by a propagating wave, high finesse for both polarization states, excellent stability, and simplicity of operation. The folded design

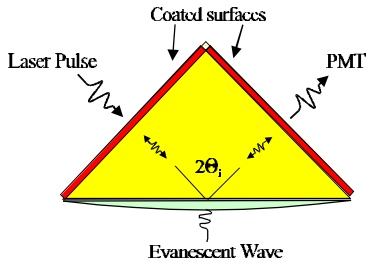

Figure 7. A monolithic, folded resonator is depicted. For $n_1>n_2$, the convex surface becomes a total internal reflection (TIR) mirror if $\grave{e}_i > \grave{e}_c = \sin^{-1}(n_2/n_1)$. The planar surfaces are coated with an ultra-high reflective dielectric coating, as employed in gas-phase CRDS cavities. The three mirror system forms a stable optical resonator for a judicious choice of mirror separation and spherical radius of curvature. The evanescent wave at the apex of TIR surface probes absorption by an ambient medium.

is formed from a monolithic solid of ultra-low-loss optical material having a refractive index n_i. The planar surfaces are ultra-high-reflective, coated surfaces, while the convex surface forms a TIR mirror. The resulting twin-waist, astigmatic resonator is stable if the spherical radius of curvature, R_C, of the convex surface and the unfolded cavity length L satisfies the condition[23],

$$0\#\left(1-\frac{L}{R_c\cos\grave{e}_i}\right)^2\#1 \qquad \textbf{(2)}$$

in the tangential plane where the effective radius of curvature $R_{eff}=R_C\cos\grave{e}_i$, which also assures stability for the sagittal plane with $R_{eff}=R_C/\cos\grave{e}_i$. The photon decay time of the cavity is also given by Eq. 1 with $L_0(\grave{u})=2(L_C + L_{surf} + L_{bulk})$, where the L_i are the per-pass coating, bulk, and TIR surface scattering loss, respectively. Ideally, L_C is dominated by residual transmission with a minimal contribution resulting from coating absorption. The surface scattering loss, L_{surf}, is minimized by super-polishing. Diffraction losses can be neglected if the resonator mode diameter is small relative to the system clear aperture. Nonspecular transmission losses can also be neglected if $\grave{e}_i ! \grave{e}_c$ 1°, depending on the curvature of the incident wavefront[4]. The sample absorption is probed by the evanescent wave, emanating from the apex of the TIR surface.

Figure 8 shows the ring-down time and round-trip intrinsic loss on opposite axes as a

function of wavelength for s- and p-polarizations for a fused-silica resonator as depicted in Figure 7 with L=3.0±0.1cm, R_C=7.5±0.1 cm, and è$_i$ =45.0°±0.08°, which employs an ultra-high-reflective coating centered at ~520 nm with an estimated loss of L_C=1.2x10^{-5} per reflection according to the manufacturer's specifications. The surface normals associated with surfaces S_1 through S_3 lie in the same plane to within ±0.08°. An excimer-pumped dye laser, which generated 20 ns, ~ 0.25 mJ laser pulses, was used without mode matching to generate the transients. The transmission through surface S_3 was monitored with a photomultiplier tube and an 8-bit digital oscilloscope. The useful bandwidth of the resonator is seen to be approximately 80 nm, limited by transmission of the coated surfaces. Note that the intrinsic loss is essentially independent of polarization. The minimum loss of 220x10^{-6} is found for s-polarization at 530 nm, with ô$_S$(530nm)=1.316 µs. By averaging 25, individually acquired ring-down times, a relative uncertainty in ô(530nm) of 0.20 % was

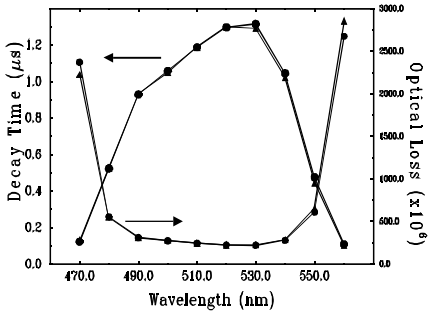

Figure 8. The intrinsic loss and ring-down time are shown on opposite axes as a function of wavelength for the monolithic cavity. The useful bandwidth of the resonator is approximately 80 nm, limited by the coating reflectivity. A minimum loss of 220 x 10^{-6} occurs at 530 nm, which is determined mainly by the bulk attenuation of fused silica. The solid circles indicate s-polarization; triangles indicate p-polarization. Note that the intrinsic losses for the two polarizations are nearly equal.

obtained, which yields a minimum detectable absorbance of $(L_{abs})_{min}$ = L_0*( )J/J) = %2L_0F$_J$/(J%N) = 4.4x10^{-7} where F$_J$ is the standard deviation and N is the number of decay times averaged.

As with the square, TIR-ring cavity, the polarization-independent finesse of the resonator in Figure 7 allows molecular orientation of an adsorbed layer and other polarization-dependent phenomena to be probed in the evanescent wave. To provide a simple demonstration of chemical detection, the adsorption of I_2 was also examined to provide a direct comparison with the square, TIR-ring cavity results. Figure 9 shows s- and p-polarized absorptions, as a function of time during exposure of the TIR surface to I_2 vapor. The TIR surface was sealed to the I_2 cell with a Viton O-ring as indicated in inset *a*. The rapid initial rise of the I_2 absorption signal results from the initial adsorption which is

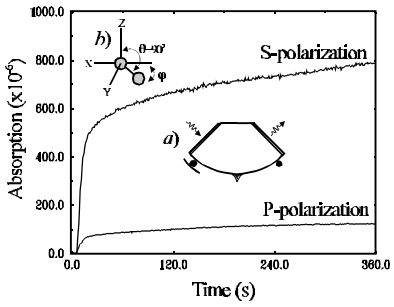

Figure 9. The absorption loss at 540 nm for s- and p-polarized cavity modes is shown as a function of time during exposure of the TIR surface to I_2 vapor at room temperature. Inset *a* indicates the geometry for sealing the TIR surface to the I_2 source by O-ring. The s-polarized absorption is found to be much larger than the p-polarized case. Since the electric field associated with an s-polarized mode lies entirely in the plane of the TIR surface, the dichroic ratio suggests that surface-bound I_2 lies flat on the surface, as indicated in the inset *b*, with È=90°, as expected from the fused-silica square-TIR- ring resonator.

expected to be rapid, based on collision frequency of I_2 molecules with the surface and the gas phase diffusion coefficient. The slow time dependence that appears after initial equilibration may result from reaction of I_2 with water or surface hydroxyl groups. Note that the s-polarized absorption is considerably stronger than the p-polarized case, while the dichroic ratio, ñ=A_s/A_p, remains essentially constant, which is identical to the square, TIR-ring resonator results, as expected.

Based on a minimum detectable absorption of $(L_{abs})_{min}=4x10^{-7}$ and an absorption cross-section of ó(540 nm)−$2x10^{-18}$ cm^2/molecule[19] for I_2, a minimum detectable coverage can be estimated from $L_{abs}=2Ãó(ù)N_s/cosè_i$, where N_s is the surface density and Ã is the field enhancement factor. Assuming $N_0=4.5x10^{14}$ sites/cm^2 as the definition of one monolayer on the SiO_2 surface, a minimum detectable coverage of 0.004% of a monolayer was found. This estimate assumes that I_2 molecules lie flat on the SiO_2 surface so that the local electric field intensity is enhanced by $Ã=(1.944)^2=3.8$, as discussed above. The gas phase absorption cross section is also employed for reasons discussed previously. An increase in sensitivity can be realized by working in spectral regions where bulk and coating losses are smaller or by reducing the size of the resonator. Improvements in sensitivity can also be expected through improvements in decay time measurement precision.

iii. Diode Laser CRDS

In order to develop a portable, inexpensive sensing technology based on EW-CRDS, the use of diode laser sources has been examined in collaboration with our commercial partner. In order to obtain the best possible ring-down time measurement precision, which optimizes sensitivity, single mode excitation is required[21]. Single-mode excitation eliminates non-exponentiality in the ring-down transient that accompanies multi-mode excitation, thereby improving decay-time-measurement precision, if employed with low-noise detection and high-resolution digitization. The use of a narrow line width source, such as a diode laser, facilitates single mode excitation and increases light throughput as the laser line width approaches the cavity line width. However, the laser diode must be optically isolated from the cavity to prevent optical feedback, which frequency shifts and distorts the diode output, rendering single mode excitation impossible. Using a linear CRDS cavity, we achieved extremely efficient (58:1), lowest-order mode (TEM_{00}), excitation with a standard, off-the-shelf diode laser (not an extended cavity diode laser system). These experiments used a 685 nm diode with a 15±5 MHZ time-averaged linewidth, which provided ample cavity output intensity (~5 µW) for detection. These results indicate that a cost effective sensing system based on EW-CRDS can be produced. Furthermore, the EW-CRDS resonator can be remotely located from the source and detector by optical fiber or all three miniature elements could be packaged on a chip.

iv. Enhancing selectivity through chemistry

The combination of EW-CRDS with chemically selective films that show molecular recognition for a particular class of molecules was also briefly examined during Project #60231. Working with collaborators at LANL, we are examining cyclodextrin films which

show selectivity for toluene, DNT, and TNT. Initial light scattering and CRDS measurements indicate that these films, which form rugged, well-ordered monolayers on super-polished surfaces, show low-scatter loss and low total attenuation. The measurements were performed using a single, coated optical flat, tilted at Brewster's angle in a linear CRDS cavity. These important preliminary results demonstrate that super-polished surfaces can be chemically modified with an organic layer without introducing large losses due to surface restructuring or contamination. The rms surface roughness of the organic layer seems to reflect the underlying substrate. These layers are in fact quite durable and can be cleaned by the same procedure used for the nascent fused-silica surface. Therefore, functionalizing the surfaces of EW-CRDS resonators to increase selectivity should be feasible.

4. Relevance, Impact, and Technology Transfer

a. Project #60231 has yielded a new chemical sensing technology that could be applicable to a wide range of DOE environmental management problems because new sensing technologies are needed as specified at the needs website.

b. Improved technologies and clean-up approaches may result from availability of new chemical characterization data at DOE sites. Clean up costs could be reduced by having an in-situ probe rather than performing sample extraction followed by ex-situ analysis. Risk reduction could result from the creation of a chemical sensing probe that can be interrogated remotely from the contaminated site. A new sensing technology that could support long-term monitoring could also help DOE comply with agreed upon regulations. Finally, this project may yield a new approach to characterizing chemically selective films that could be used by DOE.

c. The basic research performed under Project 60231 has been basic *measurement science* underlying the EW-CRDS technology. Therefore, it forms the basis for all future applications of the technology.

d. As a general chemical sensing technology, EW-CRDS could be used by many researchers in academic, government, or industrial research laboratories and could eventually become commercialized.

e. The project has made a fundamental impact since a new technology has been realized. More basic research is needed before large scale trial are justified.

f. Building collaborations requires time to plan and make funding arrangements. I have made considerable effort to build collaborations since my arrival at NIST. These efforts are beginning to yield funded interactions.

g. Project #60231 has opened up a new and rich area of research since a new tool has been developed that permits extreme sub-monolayer detection of adsorbed molecules on a surface without the need for ultra-high vacuum. The work has demonstrated that the cavity ring-

down concept can be applied to such problems.

h. EW-CRDS is in its infancy. More basic research is needed to understand the role of the nascent resonator surface in the adsorption/collection of analyte as well as for characterizing chemically selective films and silica chemistry in the environment. Other spectral regions, optical materials, and modes of operation (such as ellipsometric sensing) should also be explored. The design of a practical probe must also be accomplished in collaboration with a commercial partner.

I. Information has been sent to DOD and DTRA in response to their request. A licensing agreement with Informed Diagnostics Inc. (Sunnyvale, CA) has been negotiated, although the future direction of IDI is uncertain. Analytical Specialties Inc. (Houston, Texas) and Tiger Optics Inc. (Warrington, PA) have expressed interest in EW-CRDS. Additional information can be obtained from Terry Lynch at NIST (301-975-2691)

5. Project Productivity

The goal of Project# 60231 as stated in the original research proposal was to demonstrate the feasibility of EW-CRDS and make progress toward the development of the field-deployable device.

Project# 60231 demonstrated the feasibility of EW-CRDS through several working prototypes, which obtained or exceeded proposed sensitivity levels. Furthermore, much of the fundamental measurement science underlying EW-CRDS was elucidated, which is critical for a newly developing technology. Operation of EW-CRDS prototypes in the infrared spectral region, which was proposed contingent upon procurement of an appropriate laser source, was not carried out due to lack of capital equipment funding. (However, an appropriate source (an optical parametric oscillator) has been purchased for the renewal Project #73844.) Several designs for possible field-deployable probes have been developed. However, construction of such a prototype packaged probe was somewhat premature and deviated slightly from the NIST mission, as a lone effort. The development of a packaged probe will be considered (and is being pursued) in collaboration with a commercial and/or applied research (e.g., DOE site) partner.

There were several developments in Project #60231 that were not anticipated in the original proposal. First, the monolithic folded resonator design was conceived, fabricated, and characterized. This design will permit a field-deployable device to be constructed more easily than the TIR-ring design for applications where probing a single wavelength or narrow wavelength band is sufficient. Second, the polarization dependence of the EW-CRDS signal will likely provide some additional chemically selective information that was not fully appreciated in the initial proposal. Finally, experiments were carried out in collaboration with a commercial/CRADA partner that demonstrated the feasibility of using diode laser to achieve single cavity mode excitation. The use of diode lasers will be critical for development of a field-deployable device due to their small size, low cost, and high reliability. Achieving single

mode excitation in particular was significant since this minimizes the ring-down decay time measurement uncertainty, therefore maximizing sensitivity.

6. Personnel Supported

Only the Principal Investigator was supported by this contract throughout its duration. During a small fraction of the first year, Dr. Jeffrey W. Hudgens was supported to handle administrative responsibilities.

7. Publications

Peer-reviewed journals:

1. *Monolithic resonator for evanescent wave cavity ring-down spectroscopy*, A. C. R. Pipino, Appl. Opt. **39** (9) 1449, (2000).
2. *Ultra-sensitive surface spectroscopy with a miniature optical resonator*, A. C. R. Pipino, Phys. Rev. Lett. **83**, 3093, (1999).

Conference Proceedings:

3. A. C. R. Pipino in *Advanced Materials and Optical Systems for Chemical and Biological Detection*, M. Fallahi and B. I. Swanson, Eds., Proc. SPIE Vol. 3858, p74, Boston, Mass. (1999).
4. A. C. R. Pipino in *Advanced Sensors and Monitors for Process Industries and the Environment*, Wim A. De Groot, editor, Proc. of SPIE, Vol. 3535, p 57, Boston, Mass. 1998.

Preliminary work:

Peer-reviewed journals:

5. *Evanescent wave cavity ring-down spectroscopy as a probe of surface processes*, A.C.R. Pipino, et al., Chem. Phys. Lett. 280, 104 (1997).
6. *Evanescent wave cavity ring-down spectroscopy with a total-internal-reflection minicavity*, A. C. R. Pipino, et al., Rev. Sci. Instrum. 68, 2978 (1997).

8. Interactions

1. SPIE Conference on *Advanced Materials and Optical Systems for Chemical and Biological Detection*, Boston, Mass. (1998).
2. 1998 DOE EMSP National Meeting, Chicago, Illinois
3. Invited Talk, Northwestern University, Evanston. Illinois, March, 1999.
4. Invited Talk, Oak Ridge, TN, DOE-EMSP-sponsored.
5. 2000 DOE EMSP National Meeting, Atlanta, GA.
6. Sensors Initiative Meeting, Idaho Falls, ID, June 2000.

9. Patents

1. *Intra-cavity total reflection for high sensitivity measurement of optical properties*, A. C. R. Pipino, U.S. Patent No. 5,986,768.
2. *Intra-cavity total reflection for high sensitivity measurement of optical properties*, A. C. R. Pipino et al. U. S. Patent No. 5,943,136.
3. *Broadband intra-cavity total reflection chemical sensor*, A. C. R. Pipino, U. S. Patent No. 5,835,231, Nov. 10, 1998.

10. Future Work

Project #60231 has been renewed as Project #73844. The renewal project will explore the combination of EW-CRDS with molecular recognition chemistry, application of EW-CRDS to liquids, direct detection of TCE, alternative forms of EW-CRDS, and the use of nanostructured surfaces.

11. Literature Cited

1. A. O'Keefe and D. A. G. Deacon, Rev. Sci. Instrum. **59**, 2544 (1988).
2. M. D. Wheeler, S. M. Newman, A. J. Orr-Ewing, M. N. R. Ashfold, J. Chem. Soc. Faraday T. **94** (3), 337, (1998).
3. *Cavity-Ringdown Spectroscopy*, K. W. Busch and M. A. Busch, eds. (Oxford University Press, 1999).
4. A. C. R. Pipino, J. W. Hudgens, R. E. Huie, Rev. Sci. Instrum. **68** (8), 2978, (1997).
5. A. C. R. Pipino, J. W. Hudgens, R. E. Huie, Chem. Phys. Lett. **280**, 104 (1997).
6. A. C. R. Pipino in advanced Sensors and Monitirs for Process Industries and the Environment, Wim A. De Groot, editor, Proc. of SPIE, Vol. 3535, p 57, Boston, Mass. 1998.
7. A. C. R. Pipino in Advanced Materials and Optical Systems for Chemical and Biological detection, M. Fallahi and B. I. Swanson, Eds., Proc. SPIE Vol. 3858, p74, Boston, Mass. (1999).
8. A. C. R. Pipino, Phys. Rev. Lett. **83**(15), 3093,(1999).
9. A. C. R. Pipino, Appl. Opt. **39** (9), 1449, (2000).
10. A. C. R. Pipino and Joseph T. Hodges in Advanced Environmental and Chemical Sensing Technology, T. Vo-Dinh and Stephanus Buttgenbach, Eds., Proc. SPIE Vol. 4205, p 1, Boston, Mass. (2001).
11. N. J. Harrick, *Internal Reflection Spectroscopy*, (Interscience Publishers, New York, 1967).
12. J.A. Silver, Appl. Opt., **31**, 707-717, 1992.
13. J.M. Supplee, E.A. Whittaker, and W. Lenth, Appl. Opt., **33**, 6294-6302, 1994.
14. *Single-molecule optical detection, imaging, and spectroscopy*, Eds T. Basche et al., (VCH, Cambridge, 1997).
15. M. D. Levenson, B.A. Paldus, T.G. Spence, C.C. Harb, J.S. Harris, Jr., and R.N. Zare, Chem. Phys. Lett. **290**, 335, 1998.
16. D. Romanini and K. K. Lehmann, J. Chem. Phys. **99**, 6287-6301, (1993).
17. To dose the cavity facet with I_2 vapor, a 2 mm O.D. glass tube was packed with solid I_2

and inserted in a 5 mm O.D. x 3 mm I.D. glass tube. The concentric tubes were sealed at one end by a ground-glass joint. An O-ring groove containing a small Viton O-ring was milled into the other end of the 5 mm O.D. tube. The O-ring groove surface was polished to half-wave flatness, allowing interferometry to be used to parallelize the tube end relative to a flat cavity facet. Light contact then provided a vapor-tight seal.
18. N. L. Thompson, Harden M. McConnell, Thomas P. Burghardt, *Biophys. J.* **46**, 739, (1984).
19. J. G. Calvert and J. N. Pitts, Jr., *Photochemistry*, (John Wiley & Sons, New York, 1967).
20. G. Kortum and H. Koffer, *Ber. Bunsenges. Phys. Chem.*, **67**, 67, (1963).
21. R. D. van Zee, J. T. Hodges, and J. P. Looney, Appl. Opt. **38**, 3951 (1999).
22. *Optical Properties of Highly Transparent Solids*, Waterville Valley, NH., edited by S.S. Mitra and B. Bendow (Plenum, New York, 1975).
23. A. E. Seigmann, *Lasers*, (University Science Books, Mills Valley, CA, 1986).